American Journal of Applied Mathematics and Statistics, 2020, Vol. 8, No. 2, 43-51
Available online at http://pubs.sciepub.com/ajams/8/2/2
Published by Science and Education Publishing
DOI:10.12691/ajams-8-2-2

Study of Double Porous Layered Slider Bearing with Various Designed Stator under the Effects of Slip and Squeeze Velocity Using Magnetic Fluid Lubricant

Ramesh C Kataria[1,*], Darshana A Patel[2]

[1]Department of Mathematics, Som-Lalit Institute of Computer Applications, Ahmedabad, India
[2]Department of Mathematics and Humanities, Vishwakarma Government Engineering College, Ahmedabad, India
*Corresponding author: katariaramesh@hotmail.com

Received May 09, 2020; Revised June 11, 2020; Accepted June 18, 2020

Abstract A comparative mathematical analysis of slider bearing made up of double porous layered slider supported by solid wall with different designed stator such as convex, parallel, exponential, inclined, and secant is presented in this research paper. The study includes the effect of slip velocity as suggested by Sparrow et al. [13] at the interface of film-porous. Effects of squeeze velocity and the oblique variable magnetic field to the lower plate are considered. General form of Reynolds type equation, non-dimensional squeeze film pressure and load carrying capacity expressions are obtained. The values of non-dimensional load carrying capacity are obtained and compared among various considered designs bearings. Overall, it could be concluded that compared to others, secant pad stator slider bearing is suggested for the superior performance of the system.

Keywords: *lubrication, ferrofluid, squeeze velocity, porosity, slip velocity*

Cite This Article: Ramesh C Kataria, and Darshana A Patel, "Study of Double Porous Layered Slider Bearing with Various Designed Stator under the Effects of Slip and Squeeze Velocity Using Magnetic Fluid Lubricant." *American Journal of Applied Mathematics and Statistics*, vol. 8, no. 2 (2020): 43-51. doi: 10.12691/ajams-8-2-2.

1. Introduction

In a squeeze film bearing, *squeeze velocity* is defined as a squeeze action that takes- place, as bearing surfaces approach each other. The squeeze film lubrication plays a very considerable role in the field of industries such as in bearings, roller bearings, shaft, fluid handling systems, clutch plates, engines, gears, human skeletal joints, etc. Owing to this motivation several theoretical and experimental study from different perspective were carried out on squeeze film by numerous researchers such as circular disks by Moore [1], parallel surfaces by Gould [2], porous annular disks by Wu [3], the spherical bodies by Christensen [4], porous inclined slider bearing by Prakash and Vij [5]. With the advancement in the recent period, a number of researchers have studied various magneto-hydrodynamic (MHD) problems.

Water-based Magnetic fluid or Ferrofluid [6] is a colloidal dispersion containing ferromagnetic particles. To prevent aggregation, each magnetic particle is thoroughly coated with a suitable surfactant. While applying the magnetic field externally, ferrofluid experiences magnetic body force. As a result of this characteristic, ferrofluids (Magnetic fluids) are useful in many applications like in elastic damper, in cooling and heating cycles, in high sliding speeds, in rotating shaft seals, in loudspeakers to reduce unwanted resonances, etc. [6,7]. With the initiation of ferrofluids, many researchers have worked on ferrofluid lubrication theory to find its application on bearing systems. Effects of ferrofluid on a porous inclined slider bearing were investigated by Agrawal [8] and found that such a bearing has greater performance as compared to the viscous porous inclined slider bearing. Patel and Deheri [9] studied the effect of magnetic fluid lubricant on the squeeze films and investigated that results of the bearing in the case of secant curved plate are slightly superior to that of exponentially curved plates. Using Jenkin's model, the effects of ferrofluid on slider bearing having a circular convex pad stator were studied by Shah and Bhat [10], they concluded that film-pressure and load carrying capacity can be enlarged by the escalating the strength of the magnetic field. A comprehensive analysis of ferrofluid lubrication with some experimental studies was presented by Huang and Wang [11] and shown that; ferrofluids under the external magnetic field reduces friction and anti-wear capabilities over traditional lubricants.

In an innovative analysis, Beavers and Joseph [12] put forward an alternative boundary condition that allows a non-zero tangential velocity (called slip velocity) at the porous surface, it was found that; the consideration of slip velocity affect the bearing performance extensively.

Under the assumptions of anisotropic permeability, slip velocity at the interface of the film-porous layer, the performance of a porous composite slider bearing was analyzed by Puri and Patel [14] and concluded that the bearing had a superior load capacity and higher friction than the inclined slider bearing. Ferrofluid lubricated convex pad porous surface slider bearing with slip and squeeze velocity was studied by Shah and Bhat [15]. Under the consideration of anisotropic permeability, slip and squeeze velocities, newly designed doubled porous layered ferrofluid lubricated axially undefined journal bearing was analyzed by Shah and Patel [16]. Comparative analysis of various designed slider bearings with ferrofluid lubrication was studied by Shah and Parsania [17] and found that slider bearing design with inclined or convex pad stator surfaces gave the greater performance to the system. Recently, mathematical modeling of ferrofluid based slider bearing having convex pad stator with double porous layers attached to the slider was studied by Shah and Kataria [18] and concluded that better dimensionless load carrying capacity can be obtained. Researchers [19,20] have also analyzed the effects of ferrofluids in their study from different perspectives.

The present work attempts to investigate and evaluate the behaviour of non-dimensional load carrying capacity of various designed double porous layered slider bearings such as convex, parallel, exponential, inclined, and secant pad stator. Further, the study includes effects of slip velocity at the film-porous interface with squeeze velocity. The porous layers in the bearing are considered due to self-lubrication property and the flow in the porous region satisfies Darcy's law. A Study concerning the motion of Magnetic fluid (Ferrofluid) is based on the formulation given by R. E. Rosensweig [6]. A general Reynolds type equation is derived for the above bearing designs and non-dimensional pressure and load-carrying capacity expressions are obtained and in this connection, results are calculated.

2. Mathematical Modelling

Representation of the various designed double porous layered slider bearings with squeeze velocity $\dot{h}$ are demonstrated in Figure 1 - Figure 5.

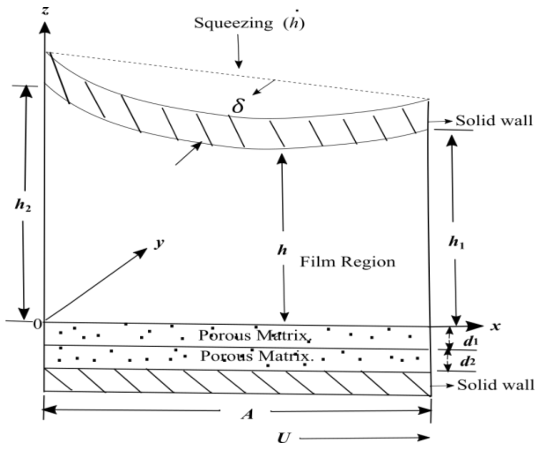

Figure 1. Double porous convex pad stator slider bearing

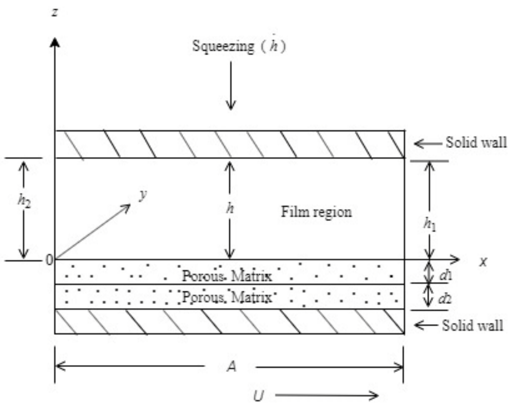

Figure 2. Double porous parallel pad stator slider bearing

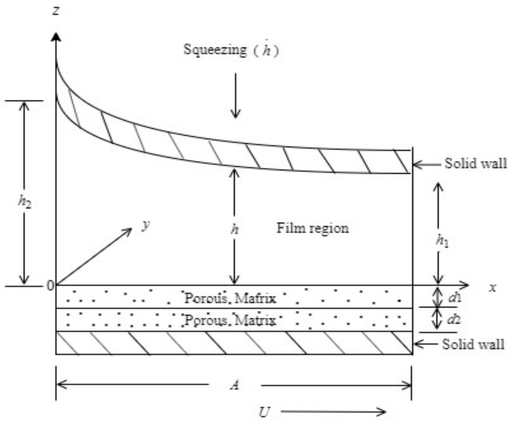

Figure 3. Double porous exponential pad stator slider bearing

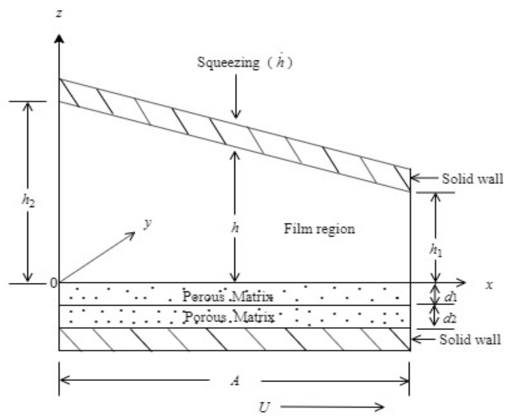

Figure 4. Double porous inclined pad stator slider bearing

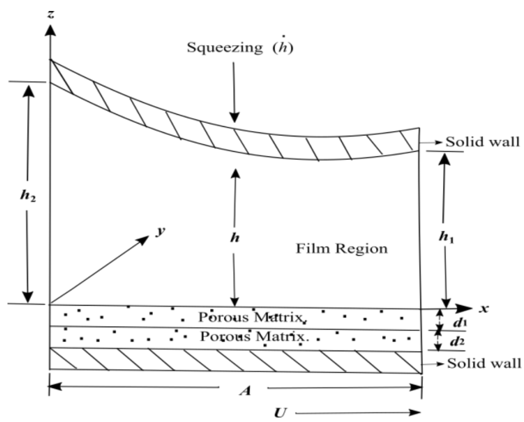

Figure 5. Double porous secant pad stator slider bearing

As shown in Figure 1 - Figure 5, in each bearing lower surface is a slider of length A and is sliding in the x-direction with consistent velocity U and width B in the y-direction, $B>>A$. A stator represents the upper surface of different profiles like convex, parallel, exponential, inclined, and secant pads. The opening between stator and slider is identified as fluid-film thickness and is filled with water-based Magnetic fluid (Ferrofluid) lubricant.

Film thickness h for each slider bearing is defined by [17] below, here h_1 and h_2 are minimum and maximum film thicknesses respectively.

• For convex pad stator:

$$h_c = \delta\left(4\left(\frac{x}{A}-\frac{1}{2}\right)^2 - 1\right) + h_1\left(a - \frac{a}{A}x + \frac{x}{A}\right); \quad a = \frac{h_2}{h_1}, 0 \le x \le A \tag{1}$$

Here δ : central thickness of the convex pad.

• For parallel pad stator:

$$h_p = h_1 = h_2, \quad 0 \le x \le A \tag{2}$$

• For exponential pad stator:

$$h_e = h_2 e^{-\frac{(x \ln a)}{A}}, \quad 0 \le x \le A \tag{3}$$

• For inclined pad stator:

$$h_i = h_2 - (h_2 - h_1)x / A, \; 0 < x \le A \tag{4}$$

• For secant pad stator:

$$h_s = h_1 \sec\left(\frac{\pi(A-x)}{2A}\right), \; 0 < x \le A. \tag{5}$$

Two porous layers of *widths* d_2 and d_1 are backed with solid wall, the lower surface-slider. Porous layer of width d_2 is attached first and then porous layer of width d_1. Also, the stator moves normally towards the lower surface-slider with the consistent velocity

$$\dot{h} = \frac{dh}{dt}, \tag{6}$$

where t is time in seconds, is called squeeze velocity.

Oblique variable magnetic field is applied to the lower surface, which vanishing at the inlet and outlet of the bearing as

$$H^2 = Kx(A-x), \tag{7}$$

where K is chosen to suit the dimensions of both sides of equation (7) which helps in getting magnetic field strength at $x = A/2$, as follows [21].

From equation (7), maximum $H^2 = 10^{-4}$ K which implies for $K = O(10^{10})$, so that $H = O(10^3)$ or $O(H) \approx 3$, here O indicates order.

For the film region, the basic flow equations [22] under the influence of magnetic field on the hydrodynamics of Ferrofluid or Magnetic fluid theory presented by R.E. Rosensweig are

$$\rho\left[\frac{\partial \mathbf{q}}{\partial t} + (\mathbf{q} \bullet \nabla)\mathbf{q}\right] = -\nabla p + \eta \nabla^2 \mathbf{q} + \mu_0 (\mathbf{M} \bullet \nabla)\mathbf{H}, \tag{8}$$

$$\nabla \times H = 0, \tag{9}$$

$$\mathbf{M} = \chi \mathbf{H}, \tag{10}$$

$$\nabla \bullet (\mathbf{H} + \mathbf{M}) = 0, \tag{11}$$

where ρ, p, η, $\mathbf{q}$, μ_0, $\mathbf{M}$, $\mathbf{H}$, χ are density, film pressure, fluid viscosity, fluid velocity, free space permeability, magnetization vector, magnetic field vector and magnetic susceptibility respectively.

And continuity equation

$$\nabla \bullet \mathbf{q} = 0, \tag{12}$$

where

$$\mathbf{q} = u\,\boldsymbol{i} + v\,\boldsymbol{j} + w\,\boldsymbol{k}, \tag{13}$$

here u, v, w are velocity components of film-fluid in directions- x, y, and z correspondingly.

Using equations (8) to (12) and assuming standard hydrodynamic lubrication for the film region, lubricant flow in the x-direction is given by

$$\frac{\partial^2 u}{\partial z^2} = \frac{1}{\eta}\frac{\partial}{\partial x}\left(p - \frac{1}{2}\mu_0 \chi H^2\right). \tag{14}$$

Here H : the magnetic field strength.

By slip boundary conditions [13]

$$u = \frac{1}{s}\frac{\partial u}{\partial z} + U; \; s = \frac{\alpha}{(k_1)^{\frac{1}{2}}}, when\ z = 0 \tag{15}$$

And

$$u = 0, \; when\ z = h, \tag{16}$$

where s: slip parameter, α: slip coefficient and k_1 : permeability of the upper porous layer. These parameters depend on the characteristics of the porous material and independent of the lubricant properties and film thickness.

Equation (14) becomes

$$u = \frac{(h-z)s}{(1+sh)}U + \left\{\frac{(z+h+sh\,z)(z-h)}{2\eta(1+sh)}\right\}\frac{\partial}{\partial x}\left(p - \frac{1}{2}\mu_0 \chi H^2\right), \tag{17}$$

Integrating equation (17) over the film region, gives

$$\int_0^h u\,dz = \frac{sh^2}{2(1+sh)}U - \frac{h^3(4+sh)}{12\eta(1+sh)}\frac{\partial}{\partial x}\left(p - \frac{1}{2}\mu_0 \chi H^2\right). \tag{18}$$

Using equation (18) in the integral form of continuity equation for the film region

$$\frac{\partial}{\partial x}\int_0^h u\,dz + w_h - w_0 = 0, \tag{19}$$

yields

$$\frac{\partial}{\partial x}\left\{\begin{array}{l}\frac{sh^2}{2(1+sh)}U \\ -\frac{h^3(4+sh)}{12\eta(1+sh)}\frac{\partial}{\partial x}\left(p-\frac{1}{2}\mu_0\,\chi H^2\right)\end{array}\right\} = w_0 - V, \quad (20)$$

as $w\big|_{z=h} = w_h = V = -\dot{h}$, which represents the effect of squeeze velocity in the downward z - direction and $w\big|_{z=0} = w_0$.

In the porous region, the components of the velocity in the x and z - directions as per Darcy's law are given by

$$\bar{u}_j = -\frac{k_j}{\eta}\frac{\partial P_j}{\partial x} + \frac{\mu_0\chi k_j}{2\eta}\frac{\partial H^2}{\partial x} \quad (21)$$

$$\bar{w}_j = -\frac{k_j}{\eta}\frac{\partial P_j}{\partial z} + \frac{\mu_0\chi k_j}{2\eta}\frac{\partial H^2}{\partial z} \quad (22)$$

respectively. Where j = 1, 2 correspond to velocity coordinates in the porous regions of widths d_1 and d_2 and permeabilities k_1 and k_2 respectively.

With the assumption of continuous flow between two porous layers in the z-direction, one obtains

$$\left[-\frac{k_1}{\eta}\frac{\partial P_1}{\partial z} + \frac{\mu_0\chi k_1}{2\eta}\frac{\partial H^2}{\partial z}\right]_{z=-d_1} = \left[-\frac{k_2}{\eta}\frac{\partial P_2}{\partial z} + \frac{\mu_0\,\chi\, k_2}{2\eta}\frac{\partial H^2}{\partial z}\right]_{z=-d_1}. \quad (23)$$

Also, at solid lower surface

$$\left[-\frac{k_2}{\eta}\frac{\partial P_2}{\partial z} + \frac{\mu_0\,\chi\, k_2}{2\eta}\frac{\partial H^2}{\partial z}\right]_{z=-(d_1+d_2)} = 0. \quad (24)$$

Substituting equations (21) and (22) in the continuity equation for the porous region

$$\frac{\partial \bar{u}}{\partial x} + \frac{\partial \bar{w}}{\partial z} = 0,$$

gives

$$\frac{\partial^2}{\partial x^2}\left(P_j - \frac{1}{2}\mu_0\chi H^2\right) + \frac{\partial^2}{\partial z^2}\left(P_j - \frac{1}{2}\mu_0\chi H^2\right) = 0, \quad j = 1, 2. \quad (25)$$

Integrating equation (25) with respect to z over the porous layer of the width d_1, yields

$$\frac{\partial}{\partial z}\left(P_1 - \frac{1}{2}\mu_0\,\chi H^2\right)\Bigg|_{z=0} - \frac{\partial}{\partial z}\left(P_1 - \frac{1}{2}\mu_0\,\chi H^2\right)\Bigg|_{z=-d_1} = -\int_{-d_1}^{0}\frac{\partial^2}{\partial x^2}\left(P_1 - \frac{1}{2}\mu_0\,\chi H^2\right)dz. \quad (26)$$

Again, integrating equation (25) with respect to z over the porous layer of the width d_2, gives

$$\frac{\partial}{\partial z}\left(P_2 - \frac{1}{2}\mu_0\,\chi H^2\right)\Bigg|_{z=-d_1} - \frac{\partial}{\partial z}\left(P_2 - \frac{1}{2}\mu_0\,\chi H^2\right)\Bigg|_{z=-(d_1+d_2)} = -\int_{-(d_1+d_2)}^{-d_1}\frac{\partial^2}{\partial x^2}\left(P_2 - \frac{1}{2}\mu_0\,\chi H^2\right)dz. \quad (27)$$

Using condition (23), equation (26) becomes

$$\frac{\partial}{\partial z}\left(P_1 - \frac{1}{2}\mu_0\,\chi H^2\right)\Bigg|_{z=0} = -\int_{-d_1}^{0}\frac{\partial^2}{\partial x^2}\left(P_1 - \frac{1}{2}\mu_0\,\chi H^2\right)dz + \frac{k_2}{k_1}\frac{\partial}{\partial z}\left(P_2 - \frac{1}{2}\mu_0\,\chi H^2\right)\Bigg|_{z=-d_1}. \quad (28)$$

By equations (24), (27) and with the help of Morgan-Cameron approximation [21], above equation (28) takes the form

$$\left[\frac{\partial}{\partial z}\left(P_1 - \frac{1}{2}\mu_0\,\chi H^2\right)\right]_{z=0} = -\left(\frac{k_1 d_1 + k_2 d_2}{k_1}\right)\frac{d^2}{dx^2}\left(p - \frac{1}{2}\mu_0\,\chi H^2\right), \quad (29)$$

Considering continuity of the normal components of velocity across the film-porous interface, gives

$$w\big|_{z=0} = \bar{w}\big|_{z=0}. \quad (30)$$

By equation (22) at z = 0, equations (29), (30) and the fact $\partial H^2/\partial z = 0$, equation (20) takes the form

$$\frac{d}{dx}\left[\left\{\begin{array}{l}12\left(k_1 d_1 + k_2 d_2\right) \\ +\frac{h^3(4+sh)}{(1+sh)}\end{array}\right\}\frac{d}{dx}\left(p - \frac{1}{2}\mu_0\,\chi H^2\right)\right] = 12\eta V + 6\eta U\frac{d}{dx}\left(\frac{sh^2}{1+sh}\right), \quad (31)$$

which is known as general form of Reynolds's equation of the considered phenomenon.

Introducing non-dimensional quantities

$$X = \frac{x}{A},\ \bar{h} = \frac{h}{h_1},\ \bar{s} = s\,h_1,\ a = \frac{h_2}{h_1},$$
$$\bar{p} = \frac{h_1^2\,p}{\eta U A},\ \bar{\delta} = \frac{\delta}{h_1},\ \mu^* = \frac{\mu_0\,\chi\, K\, A\, h_1^2}{\eta U}, \quad (32)$$
$$\psi = \frac{k_1 d_1 + k_2 d_2}{h_1^3},\ S = \frac{-2\,VA}{U\,h_1}.$$

Non-dimensional form of equations (1) - (5):

$$\bar{h}_c = 4\bar{\delta}X^2 - (a - 1 + 4\bar{\delta})X + a,\ 0 \le X \le 1,$$

$$\bar{h}_p = 1,\ 0 \le X \le 1,$$

$$\bar{h}_e = a\exp(-X\ln a)),\ 0 \le X \le 1,$$

$$\bar{h}_i = a-(a-1)X,\ 0 \le X \le 1,$$

$$\bar{h}_s = \sec\left(\frac{\pi}{2}(1-X)\right),\ 0 < X \le 1.$$

Equation (31), Reynolds's equation takes non-dimensional form as

$$\frac{d}{dX}\left[G\frac{d}{dX}\left\{\bar{p}-\frac{1}{2}\mu^* X(1-X)\right\}\right]=\frac{dE}{dX}, \quad (33)$$

where

$$G = 12\psi + \frac{\bar{h}^3(4+\bar{s}\,\bar{h})}{(1+\bar{s}\,\bar{h})},\ E=\frac{6\bar{s}\bar{h}^2}{(1+\bar{s}\bar{h})}-6SX. \quad (34)$$

Non-dimensional form of the equation (7) is

$$H^2 = KA^2X(1-X). \quad (35)$$

3. Solution

Subject to the boundary conditions

$$\bar{p}=0,\ when\ X=0,1. \quad (36)$$

Solving equation (33), the non-dimensional pressure $\bar{p}$ can be obtained as

$$\bar{p}=\frac{1}{2}\mu^* X(1-X)+\int_0^X \frac{E-Q}{G}dX,$$

$$\text{here } Q=\frac{\int_0^1 \frac{E}{G}dX}{\int_0^1 \frac{1}{G}dX}, \quad (37)$$

and $\bar{W}$ can be expressed as

$$\bar{W}=\frac{W h_1^2}{B\eta UA^2}=\frac{\mu^*}{12}-\int_0^1\frac{E-Q}{G}X\,dX,$$

$$\text{where } W=\int_0^B\int_0^A p\,dx\,dy. \quad (38)$$

4. Results and Discussion

Simpson′s 1/3rd - rule is used in the computation of non-dimensional load carrying capacity $\bar{W}$ from equation (38) for the following values [18] of the different variables.

$$h_1 = 0.05\,(\text{m}),\ h_2 = 0.10\,(\text{m}),$$

$$\chi = 0.05,\ U = 1\ (\text{ms}^{-1}),\ A = 0.15\ (\text{m}),$$

$$\eta = 0.012\ (\text{N s m}^{-2}),\ K = 10^9,\ \mu_0 = 4\pi\times10^{-7}(\text{N A}^{-2}),$$

$$\delta = 0.3(\text{m}),\ \dot{h} = 0.005\ (\text{m s}^{-1}),$$

$$d_1 = 0.01(\text{m}),\ d_2 = 0.01(\text{m}),\ \alpha = 0.1.$$

For the subsequent discussion, notations used for non-dimensional load carrying capacity of various slider bearings are as follows:

$\bar{W}_c$ - convex pad stator, $\bar{W}_p$ - parallel pad stator,

$\bar{W}_e$ - exponential pad stator, $\bar{W}_i$ - inclined pad stator,

$\bar{W}_s$ - secant pad stator.

The calculated values of $\bar{W}$ are presented as below:

Table 1 and Table 2 shows the values of $\bar{W}$, for swapping the values of k_1 and k_2, for two different cases $\dot{h}=0$ and $\dot{h}\neq 0$. It is observed that when $k_1 > k_2$, in convex pad stator slider bearing, $\bar{W}$ increases about 6.35 % in both the cases $\dot{h}=0$ and $\dot{h}\neq 0$ as compared to $k_1 < k_2$. When $k_1 < k_2$, $\bar{W}$ increases about 1.76 % in exponential pad stator slider bearing, 1.79 % in inclined pad stator slider bearing, and 3.87% in secant pad stator slider bearing for $\dot{h}=0$ and $\dot{h}\neq 0$ as compared to $k_1 > k_2$. When $\dot{h}=0$, if we swap the values of k_1 and k_2 in parallel pad stator slider bearing, the values of $\bar{W}$ remains same.

Table 3 and Table 4 present the values of $\bar{W}$ by considering two same values of k_1 and k_2 for two different cases $\dot{h}=0$ and $\dot{h}\neq 0$. It is observed that when $k_1 = k_2 = 0.0001$, $\bar{W}$ increases about 113% for convex pad stator slider bearing, 22% for exponential pad stator slider bearing, 22% for inclined pad stator slider bearing and 18% for secant pad stator slider bearing in both the cases for $\dot{h}=0$ and $\dot{h}\neq 0$ as compared to $k_1 = k_2 = 0.01$. When $k_1 = k_2 = 0.0001$, $\bar{W}$ increases about 2.46% for parallel pad stator slider bearing as compared to $k_1 = k_2 = 0.01$ for $\dot{h}\neq 0$.

Table 5 and Table 6 present the values of $\bar{W}$ by considering same widths of both the porous layers with respect to $k_1 = k_2 = 0.01$, assuming $\dot{h}=0$ and $\dot{h}\neq 0$. It shows $\bar{W}$ is maximum when $d_1 = 0$ and $d_2 = 0$. But with the attachment of double porous layers, maximum $\bar{W}$ can be obtained for small sizes of both the porous layers for exponential, secant and inclined pad stator slider bearing for $\dot{h}=0$, $\dot{h}\neq 0$ and $k_1 = k_2 = 0.01$. Thus, we can say that for small permeability, $\bar{W}$ increases. Also, $\bar{W}$ remains the same for parallel pad stator slider bearing when $\dot{h}=0$.

Table 7 and Table 8 show $\bar{W}$ increases for exponential, inclined and secant slider bearing when widths of both the porous layer are small. Also, for distinct decreasing values of d_1 and d_2, $\bar{W}$ remains same for $\dot{h}=0$, but it increases for $\dot{h}\neq 0$ in parallel pad stator slider bearing, while $\bar{W}$ decreases for convex pad stator slider bearing for both $\dot{h}=0$ and $\dot{h}\neq 0$.

Table 9 and Table 10 present the values of $\bar{W}$ by considering the same widths of both the porous layer with respect to k_1 = 0.0001 and k_2 = 0.1 considering $\dot{h}=0$ and $\dot{h}\neq 0$. It shows $\overline{W}$ increases for exponential, inclined and secant pad stator slider bearing for k_1 = 0.0001, k_2 = 0.1 and $\dot{h}=0$, $\dot{h}\neq 0$. So, we can say that, when the permeability of upper porous layer is small as compared to lower porous layer then $\overline{W}$ increases for exponential, inclined and secant pad stator slider bearing. For different widths d_1 and d_2, there is no change in non-dimensional load capacity for parallel pad stator slider bearing for $\dot{h}=0$.

Table 1. $\overline{W}$ by swapping the values of k_1 and k_2 taking $\dot{h}\neq 0$

k_1	k_2	$\overline{W}_c$	$\overline{W}_p$	$\overline{W}_e$	$\overline{W}_i$	$\overline{W}_s$
0.1	0.0001	0.1621569	0.1638404	0.1640247	0.1640291	0.1642217
0.0001	0.1	0.1524624	0.1638419	0.1669208	0.1669700	0.1705878
% increase in $\overline{W}$		6.35	0.0009	1.77	1.79	3.88

Table 2. $\overline{W}$ by swapping the values of k_1 and k_2 taking $\dot{h}=0$

k_1	k_2	$\overline{W}_c$	$\overline{W}_p$	$\overline{W}_e$	$\overline{W}_i$	$\overline{W}_s$
0.1	0.0001	0.1620510	0.1636905	0.1638891	0.1638946	0.1641476
0.0001	0.1	0.1523362	0.1636905	0.1667791	0.1668291	0.1705025
% increase in $\overline{W}$		6.38	0.000	1.76	1.79	3.87

Table 3. $\overline{W}$ for same values of k_1 and k_2 considering $\dot{h}\neq 0$

k_1	k_2	$\overline{W}_c$	$\overline{W}_p$	$\overline{W}_e$	$\overline{W}_i$	$\overline{W}_s$
0.0001	0.0001	0.3385819	0.1683898	0.2031797	0.2028627	0.1969178
0.01	0.01	0.1592045	0.1643411	0.1661153	0.1661417	0.1664758
% increase in $\overline{W}$		112.67	2.46	22.31	22.10	18.28

Table 4. $\overline{W}$ for same values of k_1 and k_2 considering $\dot{h}=0$

k_1	k_2	$\overline{W}_c$	$\overline{W}_p$	$\overline{W}_e$	$\overline{W}_i$	$\overline{W}_s$
0.0001	0.0001	0.3386675	0.1636905	0.2013517	0.2011534	0.1960181
0.01	0.01	0.1588051	0.1636905	0.1656497	0.1656887	0.1662517
% increase in $\overline{W}$		113.26	0.00	21.55	21.40	17.90

Table 5. $\overline{W}$ for same values of d_1 and d_2 with $k_1 = k_2 = 0.01$ and $\dot{h}=0$

d_1	d_2	$\overline{W}_c$	$\overline{W}_p$	$\overline{W}_e$	$\overline{W}_i$	$\overline{W}_s$
3	3	0.1636797	0.1636905	0.1637018	0.1637021	0.1637828
1	1	0.1636563	0.1636905	0.1637242	0.1637252	0.1639256
0.1	0.1	0.1691361	0.1636905	0.1640055	0.1640143	0.1646607
0.05	0.05	0.1591652	0.1636905	0.1642785	0.1642940	0.1650338
0	0	0.1746165	0.1636905	0.1690870	0.1691025	0.1684826

Table 6. $\overline{W}$ for same values of d_1 and d_2 considering $k_1 = k_2 = 0.01$ and $\dot{h}\neq 0$

d_1	d_2	$\overline{W}_c$	$\overline{W}_p$	$\overline{W}_e$	$\overline{W}_i$	$\overline{W}_s$
3	3	0.1636824	0.1636931	0.1637044	0.1637047	0.1637850
1	1	0.1636643	0.1636983	0.1637320	0.1637330	0.1639319
0.1	0.1	0.1691383	0.1637671	0.1640783	0.1640867	0.1647048
0.05	0.05	0.1592946	0.1638407	0.1644149	0.1644294	0.1651095
0	0	0.1726714	0.1675794	0.1704452	0.1703622	0.1691509

Table 7. $\overline{W}$ **for same sizes of** d_1 **and** d_2 **taking** $k_1 = 0.1$, $k_2 = 0.0001$ **and** $\dot{h} = 0$

d_1	d_2	$\overline{W}_c$	$\overline{W}_p$	$\overline{W}_e$	$\overline{W}_i$	$\overline{W}_s$
3	3	0.1636900	0.1636905	0.1636913	0.1636913	0.1636980
1	1	0.1636889	0.1636905	0.1636928	0.1636929	0.1637120
0.1	0.1	0.1636715	0.1636905	0.1637132	0.1637139	0.1638296
0.05	0.05	0.1636449	0.1636905	0.1637352	0.1637366	0.16390066
0	0	0.1670543	0.1636905	0.1654536	0.1654607	0.1652634

Table 8. $\overline{W}$ **for same sizes of** d_1 **and** d_2 **with** $k_1 = 0.1$, $k_2 = 0.0001$ **and** $\dot{h} \neq 0$

d_1	d_2	$\overline{W}_c$	$\overline{W}_p$	$\overline{W}_e$	$\overline{W}_i$	$\overline{W}_s$
3	3	0.1636905	0.1636910	0.1636985	0.1636918	0.1636918
1	1	0.1636904	0.1636921	0.1636944	0.1636944	0.1637133
0.1	0.1	0.1636878	0.1637060	0.1637286	0.1637293	0.1638410
0.05	0.05	0.1636803	0.1637215	0.1637655	0.1637668	0.1639210
0	0	0.1649784	0.1674848	0.1667642	0.1666749	0.1659072

Table 9. $\overline{W}$ **for same sizes of** d_1 **and** d_2 **considering** $k_1 = 0.0001$, $k_2 = 0.1$**and** $\dot{h} = 0$

d_1	d_2	$\overline{W}_c$	$\overline{W}_p$	$\overline{W}_e$	$\overline{W}_i$	$\overline{W}_s$
3	3	0.1633068	0.1636905	0.1637019	0.1637021	0.1637551
1	1	0.1626256	0.1636905	0.1637247	0.1637253	0.1638805
0.1	0.1	0.1584162	0.1636905	0.1640289	0.1640350	0.1652169
0.05	0.05	0.1569106	0.1636905	0.1643601	0.1643719	0.1662550
0	0	0.3354656	0.1636905	0.2024224	0.2021947	0.1966901

Table 10. $\overline{W}$ **for same sizes of** d_1 **and** d_2 **considering** $k_1 = 0.0001$, $k_2 = 0.1$ **and** $\dot{h} \neq 0$

d_1	d_2	$\overline{W}_c$	$\overline{W}_p$	$\overline{W}_e$	$\overline{W}_i$	$\overline{W}_s$
3	3	0.1633074	0.1636910	0.1637024	0.1637026	0.1637556
1	1	0.1626272	0.1636921	0.1637262	0.1637269	0.1638819
0.1	0.1	0.1584308	0.1637061	0.1640444	0.1640504	0.1652293
0.05	0.05	0.1569386	0.1637215	0.1643907	0.1644025	0.1662778
0	0	0.3355169	0.1686905	0.2043056	0.2039525	0.1976204

Table 11. Comparative effect of conventional lubricant and magnetic fluid on $\overline{W}$ **for** $k_1 = k_2 = 0.0001$ **and different values of** μ^* **and** $\dot{h}$

	$\dot{h} = 0$		% increase in $\overline{W}$ for $\mu^* \neq 0$	$\dot{h} \neq 0$		% increase in $\overline{W}$ for $\mu^* \neq 0$
	$\mu^* = 0$ (Using conventional lubricant or without using magnetic fluid lubricant)	$\mu^* \neq 0$ (Using magnetic fluid lubricant)		$\mu^* = 0$ (Using conventional lubricant or without using magnetic fluid lubricant)	$\mu^* \neq 0$ (Using magnetic fluid lubricant)	
$\overline{W}_c$	0.1749770	0.3386675	93.55%	0.1748914	0.3385819	93.59%
$\overline{W}_p$	0.0000000	0.1636905	16.36%	0.0046993	0.1683898	3483.29%
$\overline{W}_e$	0.0376612	0.2013517	434.64%	0.0394892	0.2031797	414.52%
$\overline{W}_i$	0.0374629	0.2011534	436.94%	0.0391722	0.2028627	417.87%
$\overline{W}_s$	0.0323276	0.1960181	506.35%	0.0332273	0.1969178	492.64%

Thus, the maximum $\overline{W}$ for all shapes of the bearing can be obtained when $d_1 = d_2 = 0$, *i.e.* when there is no porous region on the slider for $\dot{h} = 0$ and $\dot{h} \neq 0$. In general, when the width of porous region is small, the load capacity increases, as the presence of porous layer provides an alternative path for the fluid-flow resulting in an increase in sinkage rate.

Table 11 shows, the comparative effect of conventional lubricant and magnetic fluid on $\overline{W}$ by considering two same values of k_1 and k_2 for $\dot{h}=0$ and $\dot{h}\neq 0$. It is observed that the use of magnetic fluid as lubricant $\overline{W}$ increases more as compared to conventional lubricant. And it is found that convex pad stator slider bearing is having superior load-supporting capacity when $\mu^*\neq 0$ as compared to $\mu^*=0$. For $\dot{h}=0$ when $\mu^*=0$, then $W_c=0.1749770$ and when $\mu^*\neq 0$, then $W_c=0.3386675$. Therefore, the increase rate of W_c is almost 93.55% when $\mu^*\neq 0$ as compared to $\mu^*=0$. Similarly, for $\dot{h}\neq 0$ when $\mu^*=0$, $W_c=0.1748914$ and when $\mu^*\neq 0$, $W_c=0.3385819$. Therefore, the increase rate of $\overline{W}$ is almost 93.59% when $\mu^*\neq 0$ as compared to $\mu^*=0$.

It is also observed from Table 11, that the using magnetic fluid as lubricant $\overline{W}$ increases more, up to 434.64% for exponential pad stator slider bearing, 436.94% for inclined pad stator slider bearing and 506.36% for secant pad stator slider bearing as compared to conventional lubricant for k_1 = k_2 =0.0001 and $\dot{h}=0$. For $\dot{h}\neq 0$ and $\mu^*\neq 0$, $\overline{W}$ increases about 414.52% for exponential pad stator slider bearing, 417.87% for inclined pad stator slider bearing and 492.64% for secant pad stator slider bearing as compared to conventional lubricant.

In the absence of squeeze velocity and magnetic fluid lubricant, model does not support any load to parallel pad stator slider bearing. Squeeze velocity has significant effect on the bearing design system.

5. Conclusions

We noted the following results from the analysis.

1. During the course of the investigation, it is observed that the constant magnetic field does not enhance $\overline{W}$ in this model, as $\partial H/\partial x=0$ in equation (14).
2. Among all the bearing designs, secant slider bearing supports maximum $\overline{W}$ for two different cases of permeability *i.e.* $k_1 < k_2$ and $k_1 > k_2$ when $\dot{h}=0$.
3. Secant slider bearing has maximum $\overline{W}$ than other bearings when $k_1 < k_2$ for $\dot{h}\neq 0$.
4. Almost same behavior is obtained for exponential and inclined pad stator slider bearing, when $k_1 < k_2$, $k_1 > k_2$ and $k_1 = k_2$ for $\dot{h}=0$.
5. Among all the bearing designs, $\overline{W}$ increases for both $\dot{h}=0$ and $\dot{h}\neq 0$ when k_1 = k_2 = 0.0001 as compared to $k_1 = k_2$= 0.01.
6. $\overline{W}$ increases when the permeability of the upper porous layer is small as compared to the lower porous layer.
7. Better load carrying capacity is obtained when widths d_1 and d_2 of upper and lower porous layers are small for exponential, inclined and secant pad stator slider bearing for both $\dot{h}=0$ and $\dot{h}\neq 0$.

Thus, for the superior performance of the system, it is recommended to design secant pad stator slider bearing when $\dot{h}=0$ and $\dot{h}\neq 0$.

Nomenclature

a	$\frac{h_2}{h_1}$
A	Bearing length (m)
B	Bearing breadth (m)
d_1, d_2	Widths of the porous regions (m)
h	Fluid film thickness (m)
$\overline{h}$	Non-dimensional film thickness
h_1, h_2	Minimum and maximum values of h
$\dot{h}$	dh/dt, squeeze velocity (m/s)
H	Strength of variable magnetic field
H	Magnetic field vector
K	Quantity as defined in eq. (7)
k_1, k_2	Permeability of the porous regions (m^2)
M	Magnetization vector
p	Film pressure (N/m^2)
P	Fluid pressure in the porous region (N/m^2)
q	Fluid velocity vector
s	Slip parameter (1 / m)
$\overline{s}$	Non dimensional slip parameter
t	Time (s)
u, v, w	Components of film fluid velocity in x, y and z -directions (m/s)
U	Velocity of slider (m/s)
$\overline{u}_j, \overline{w}_j$	Darcy's velocity components in the x and z -directions respectively
W	Load-carrying capacity (N)
$\overline{W}$	Non-dimensional load-carrying apacity as defined in eq. (38)
x, y, z	Cartesian co-ordinates (m)
η	Fluid viscosity ($N\,s/m^2$)
μ_0	Free space permeability (N/A^2)
α	Slip constant
ρ	Fluid density ($N\,s^2/m^4$)
χ	Magnetic susceptibility
μ^*	Non-dimensional magnetization parameter as defined in eq. (32)

References

[1] Moore, D. F., "A review of squeeze films," *Wear*, 8(4), 245-263, 1965.

[2] Gould, P., "Parallel surface squeeze films: the effect of the variation of the viscosity with temperature and pressure," *J. Lubr. Technol*., 89(3), 375-380, 1967.

[3] Wu, H., "Squeeze-film behavior for porous annular disks," *J. Lubr. Technol*., 92(4), 593-596, 1970.

[4] Christensen, H., "Elastohydrodynamic theory of spherical bodies in normal approach," *J. Lubr. Technol.*, 92(1), 145-153, 1970.

[5] Prakash, J. and Vij, S.K., "Hydrodynamic lubrication of a porous slider," *J. Mech. Eng. Sci.*, 15(3), 232-234, 1973.

[6] Rosensweig, R.E., *Ferrohydrodynamics*, Cambridge University Press, New York, 1985.

[7] Goldowsky, M., "New methods for sealing, filtering, and lubricating with magnetic fluids," *IEEE trans. on Magnetics,* 16 (2), 382-386, 1980.

[8] Agrawal, V.K., "Magnetic fluid based porous inclined slider bearing," *Wear*, 107 (2), 133 -139, 1986.

[9] Patel, R.M. and Deheri, G.M., "Magnetic fluid based film between two curved plates lying along the surfaces determined by secant functions," *Indian J. of Eng. and Mater. Sci.*, 9, 45-48, 2002.

[10] Shah, R.C. and Bhat M.V., "Ferrofluid lubrication of a slider bearing with a circular convex pad," *J. Natl Sci Found of Sri Lanka*, 32(3&4), 139-148, 2004.

[11] Huang, W. and Wang, X., "Ferrofluids lubrication: a status report," *Lubr. Sci.*, 28(1), 3-26, 2016.

[12] Beavers, G.S. and Joseph, D.D., "Boundary conditions at a naturally permeable wall," *J. Fluid Mech.*, 30, 197-207, 1967.

[13] Sparrow, E.M., Beavers, G.S. and Hwang, I.T., "Effect of velocity slip on porous-walled squeeze films," *J. Lubr. Technol.*, 94(3), 260-265, 1972.

[14] Puri, Vinay and Patel, C.M., "Analysis of a composite porous slider bearing with anisotropic permeability and slip velocity," *Wear*, 84**(**1), 33-38, 1983.

[15] Shah, R.C. and Bhat, M.V., "Ferrofluid lubrication of a porous slider bearing with a convex pad surface considering slip velocity," *Int J Appl Electrom Mecha.*, 20(1), 1-9, 2004.

[16] Shah, R.C. and Patel, D.B., "Mathematical analysis of newly designed ferrofluid lubricated doubled porous layered axially undefined journal bearing with anisotropic permeability, slip velocity and squeeze velocity," Int. J. Fluid Mech. Res., 40(5), 446-454, 2013.

[17] Shah, R.C. and Parsania M. M., "Comparative study of parallel plate slider bearing with other slider bearings using magnetic fluid as lubricant," *Am. J. Math. Stat.*, 3(4), 179-189, 2013.

[18] Shah, R.C. and Kataria, R. C., "Mathematical Analysis of newly designed two porous layers slider bearing with a convex pad upper surface considering slip and squeeze velocity using ferrofluid lubricant," Int. J. Math. Model. *Comput*., 4(2), 93-101, 2014.

[19] Shah, R.C. and Patel, D. A., "On the ferrofluid lubricated squeeze film characteristics between a rotating sphere and a radially rough plate," *Meccanica*, 51**(**8), 1973-1984, 2016.

[20] Shah, R.C., Kataria, R. C. and Patel, D. A., "Ferrofluid lubricated porous squeeze-film bearing with the modified condition of pressure continuity at the film-porous interface," *Tribol.* Online, 14(3), 123-130, 2019.

[21] Shah, R. C. and Bhat, M.V., "Ferrofluid lubrication equation for porous bearing considering anisotropic permeability and slip velocity," *Indian J. Eng. Mater. Sci.*, 10, 277-281, 2003.

[22] Shah, R. C. and Bhat, M. V., "Analysis of a porous exponential slider bearing lubricated with a ferrofluid considering slip velocity," *J. Braz. Soc. Mech. Sci. and Eng.*, 25(3), July/Sept. 2003.